Atmos. Meas. Tech. Discuss., 5, 61–96, 2012
www.atmos-meas-tech-discuss.net/5/61/2012/
doi:10.5194/amtd-5-61-2012

Atmospheric Measurement Techniques Discussions

Correcting spaceborne reflectivity measurements for application in solar ultraviolet radiation levels calculations at ground level

P. N. den Outer[1], A. van Dijk[1], H. Slaper[1], A. V. Lindfors[2], H. De Backer[3], A. F. Bais[4], U. Feister[5], T. Koskela[2], and W. Josefsson[6]

[1]National Institute for Public Health and the Environment, Bilthoven, The Netherlands
[2]Finnish Meteorological Institute, Helsinki, Finland
[3]Royal Meteorological Institute of Belgium, Uccle, Belgium
[4]Aristotle University of Thessaloniki, Thessaloniki, Greece
[5]Deutscher Wetterdienst, Lindenberg, Germany
[6]Swedish Meteorological and Hydrological Institute, Norrköping, Sweden

Received: 9 December 2011 – Accepted: 19 December 2011 – Published: 4 January 2012

Correspondence to: P. N. den Outer (peter.den.outer@rivm.nl)

Published by Copernicus Publications on behalf of the European Geosciences Union.

Abstract

The Lambertian Equivalent Reflection (LER) produced by satellite-carried instruments is used to determine cloud effects on ground level UltraViolet (UV) radiation. The focus is on data use from consecutive operating instruments: the Total Ozone Mapping Spectrometers (TOMS) flown on Nimbus 7 from 1979 to 1992, TOMS on Earth Probe from 1996 to 2005, and the Ozone Monitoring Instrument (OMI) flown on Aura since 2004. The LER data produced by TOMS on Earth Probe is only included until 2002. The possibility to use the Radiative Cloud Fraction (RCF)-product of OMI is also investigated. A comparison is made with cloud effects inferred from ground-based pyranometer measurements at over 83 World Radiation Data Centre stations. Modelled UV irradiances utilizing LER data are compared with measurements of UV irradiances at eight European low elevation stations. The LER data set of the two TOMS instruments shows a consistent agreement, and the required corrections are of low percentage i.e. 2–3 %. In contrast, the LER data of OMI requires correction of 7–10 %, and a solar angle dependency therein is more pronounced. These corrections were inferred from a comparison with pyranometer data, and tested using the UV measurements. The RCF product of OMI requires a large correction but can then be implemented as a cloud effect proxy. However, a major drawback of RCF is the large number of clipped data, i.e. 18 %, and results are not better than those obtained with the corrected LER product of OMI. The average reduction of UV radiation due to clouds for all sites together indicate a small trend: a diminishing cloudiness, in line with ground-based UV observations. Uncorrected implementation of LER would have indicated the opposite. An optimal field of view of 1.25° was established for LER data to calculate UV radiations levels. The corresponding area can be traversed within 5–7 h at the average wind speeds found for the West European continent.

AMTD

5, 61–96, 2012

1 Introduction

The amount of ozone in the stratosphere and the presence of clouds are atmospheric properties that mostly determine the level of solar UltraViolet (UV) radiation at the earth surface. Long-term trends or changes in these particular atmospheric properties therefore have direct consequences for UV radiation exposure and hence, important implications to health and ecosystems (UNEP, 2010; WMO, 2011). To determine the transmission of solar radiation through the atmosphere, measuring the downwelling UV radiation with ground-based instruments that are facing up is inherently a more accurate approach than measuring reflections at the top of the atmosphere. However, only spaceborne instruments can capture the full regional and global-scale effects owing to UV radiation exposure. The time scales of UV radiation-related health effects and processes like ozone depletion and recovery exceed, however, the life span of spaceborne instruments. Therefore, these types of analyses will generally be based on data from instruments that have operated sequentially. This puts high demands not only on an absolute calibration but even more on the instrument-to-instrument calibrations.

A minimal requirement to determine the ground level UV radiation using spaceborne observations is access to total column ozone data and a cloud effect proxy. Improvements to the derived UV radiation levels can then be made by incorporating (local) ancillary data, e.g. data on aerosols optical depth and snow cover, or profile information. Total column ozone has been monitored continuously from space since the Total Ozone Mapping Spectrometer (TOMS) on NIMBUS 7 started in 1978, except for a data gap between 1993 and 1996. In the recent past, there were simultaneously operating instruments: TOMS on Earth Probe, Global Ozone Monitoring Experiment (GOME) (Burrows et al., 1999), Scanning Imaging Absorption Spectrometer for Atmospheric Cartography (SCIAMACHY) (Bovensmann et al., 1999), Ozone Monitoring Instrument (OMI) (Levelt et al., 2006) and GOME-2 (http://www.esa.int/esaME/gome-2.html). Differences between the instruments exists in the number of overpasses per day, overpass times of

AMTD
5, 61–96, 2012

the spacecrafts, and instrument properties like field of view, view angles, spectral resolution, wavelength range, etc. This leads to a variety of data products in addition to total column ozone that can be inferred from these instruments. Data products of OMI are accessible through the AURA validation centre WebPages (see reference AURA). The Tropospheric Emission Monitoring Internet Service (www.temis.nl) gives links to SCIAMACHY, GOME and GOME-2 data products. Although not all instruments have daily global coverage, advanced data assimilation or "now casting" provides in global coverage for every 6 h for GOME and SCIAMACHY data (Eskes et al., 2003). A merged data set for the whole spaceborne observation period has been constructed for the total column ozone (Van der A et al., 2010).

Unfortunately, in contrast to total column ozone, spaceborne cloud products have a much lower uniformity. This could well be the consequence of cloud products often being an intermediate product in, for instance, trace gas retrievals. The variety in cloud products and the wavelength for which they have been derived, make an assimilation of global cloud fields difficult, and thereby long-term analysis on the UV radiation related adverse and positive effects. Assimilation is also hampered by the much higher intrinsic spatial and temporal variability of clouds than that of total column ozone.

Many studies have demonstrated the ability (and limitations) of spaceborne measurements to assess the ground level UV radiation (Eck et al., 1995; Herman et al., 1997; Kalliskota et al., 2000; Matthijsen et al., 2000; Krotkov et al., 2001; Kazantzidis et al., 2006; Arola et al., 2009; Kazadzis et al., 2009). Cloud effects for summer periods derived from the International Satellite Cloud Climatology Project (ISCCP) data – cloud fraction and optical depth – perform a little worse than derived from the Lambertian Equivalent Reflection (LER) (Matthijsen et al., 2000; Williams et al., 2004). Daily sums of UV irradiance using ISCCP data indicates a similar good performance with respect to the standard deviations (Lindfors et al., 2009). Herman et al., (2009) made a long-term analysis of the LER data set on a global scale, also including data from the Sea-viewing Wide Field-of-view Sensor (Barnes et al., 2001). Diurnal variations were investigated showing that generally LER above sea peaks in the morning, in contrast

AMTD
5, 61–96, 2012

to LER over land that peaks in the afternoon (Labow et al., 2011). Herman (2010) made a global analysis of the UV irradiance using 30 yr of satellite data, showing that zonal average UV irradiance increased significantly since 1979, except for the equatorial band.

In this paper, we make an assessment of available LER data from three consecutive operating instruments: the Total Ozone Mapping Spectrometers (TOMS) flown on Nimbus 7 and TOMS flown on Earth Probe, and the Ozone Monitoring Instrument (OMI) flown on EOS-Aura. We investigate how well ground level UV irradiance is modelled by applying LER, and focus on the differences between these three instruments in the determined cloud effects for UV irradiance. In essence the performed analysis is a comparison of satellite-derived Cloud Modification Factors (CMFs) versus ground-based CMFs, where the latter is inferred from measured daily sums of global solar radiation or from measured UV irradiance.

The reason to focus on the LER-product is twofold. First, it is the longest and readily available data record for a cloud effect proxy, and secondly, non-radiative cloud parameters like cloud octas and cloud fraction are less suitable to infer cloud effects on UV irradiance because the radiation transfer has a complex nature with a large fraction of Rayleigh scattered radiation and a strong wavelength dependent absorption mean free path. Additionally, important health topics currently under debate are UV-induced production of vitamin-D and its attributed beneficial effects versus the instances of skin cancer caused by UV radiation. Since both put different weights on the UV spectrum, stand-alone cloud effect proxies are required to address this topic.

In Sect. 2, we discuss the data sets we used for this paper and present information on the sources and restrictions we made. In Sect. 3, an investigation is presented on the optimal field of view when applying LER data as a cloud effect proxy for the ground level UV irradiance. An assessment of consistency and a search for improvements is then carried out in Sect. 4 by a comparison with pyranometer measurements gathered at the World Radiation Data Centre. Pyranometers are chosen as they provide a much higher spatial density and are available for a much longer time period than ground-based UV

AMTD
5, 61–96, 2012

irradiance measurements. The validity of the found improvements is tested through a comparison with ground-based UV irradiance measurements of eight European sites.

2 Utilized data sets and used definitions

We will not engage with temporal resolutions that are higher than one value per day, any available higher resolution data will first be integrated to a daily value. The term "UV irradiance" denotes the erythemally weighted spectral irradiance at ground level integrated over wavelength (McKinley and Diffey, 1987). A daily UV sum will be the UV irradiance integrated over a day. A modelled daily UV sums is calculated in a two step process: first, an UV radiation transfer model (cprm.acd.ucar.edu/Models/TUV) delivers the clear sky daily UV sum, based on ozone and local ancillary data like aerosol loading, ground albedo, height above sea level etc. Next, the clear sky daily UV sum is multiplied by a Cloud Modification Factor F to obtain the cloudy sky daily UV sum. In this paper, F will always represent a factor to be applied to daily UV sums, and hence applies to ultraviolet wavelengths. F typically ranges from 0.1 to 1.1. It can be inferred from ground-based measurements, F_{gb}, e.g. Global Solar Irradiance (GSI) (Calbó et al., 2005), or from spaceborne data, F_{sat}, e.g. LER (Eck et al., 1995; Herman et al., 1997; Krotkov et al., 2001).

Because we want to evaluate only the cloud information of the satellite measurements, we use ground-based ozone data and other available local ancillary measurements to calculate the so-called spaceborne UV sums or spaceborne UV irradiances. For the same reason, we do not incorporate in this study the pre-calculated UV products of TOMS OMI because it tends to overestimate the actual erythemally weighted UV irradiance (Tanskanen et al., 2007).

AMTD
5, 61–96, 2012

2.1 Lambertian equivalent reflectivity and radiative cloud fraction

We utilize LER produced by TOMS flown on Nimbus 7, from 1979 to 1992, TOMS on Earth Probe, available from 1996 to 2005, and by OMI on AURA, from 2004 to 2008. LER produced by TOMS is used until the year 2002, after 2002 calibration problems of this instrument emerge (Van Dijk et al., 2008; Herman et al., 2009). LER basically returns the fraction of excess amount of radiation reflected by the atmosphere without the Rayleigh scattering contribution, and is measured in the UV-A range: 331 nm. LER is expressed as a percentage and runs from what should be the ground albedo, a few percent, to 100 %. Occasionally, values slightly over 100 % are listed as well. For convenience, we apply a multiplication by 0.01 to all LER values, F_{sat} is then essentially 1-LER, cf. Eck et al. (1995) who applied a binary ground albedo correction, and Herman et al. (2009) who give an expression of all multiple reflection between ground, clouds and scattering atmosphere. In the same paper, a more elaborate discussion on the LER retrieval is also presented. Besides the LER data, we will additionally analyse the Radiative Cloud Fraction (RCF). RCF is the "fraction of radiation detected by the satellite that has been scattered by clouds, i.e. the effective cloud fraction times the assumed cloudy radiance divided by the measured radiance". RCF because of its definition is an interesting product and, although not intended as a cloud effect proxy for radiation transfer calculations, it is tested in the same manner. Also, RCF data has been the replacement for the LER data set of OMI for some time. More information on RCF can be found on the Space-Based Measurements of Ozone and Air Quality site (http://ozoneaq.gsfc.nasa.gov/).

The available data of TOMS flown on Nimbus 7 and on Earth Probe is one data field per day on a latitude longitude grid of $1.0^{\circ} \times 1.25^{\circ}$. Overpass data for a long list of locations of meteorological stations is also produced. As OMI has been adopted as the successor of Earth Probe TOMS, its products have inherited the same format, although the delivered grid sizes has changed over time. First the format of the ozone and LER data was on the same $1.0^{\circ} \times 1.25^{\circ}$ grid as the TOMS data, to day it is delivered on

AMTD
5, 61–96, 2012

a $1.0^\circ \times 1.0^\circ$ grid. Additionally, a high resolution grid of $0.25^\circ \times 0.25^\circ$ is produced. The overpass data sets of OMI, for the same set of locations as Nimbus 7 and Earth Probe TOMS, contain also the multiple overpasses for the same day, up to three for the Polar Regions. Details of used data sets, versions, and references to detailed description of the satellite carried instruments are given in Table 1. Although some difference exists between the gridded and overpass data versions, generally from our perspective the use of either does not lead to different conclusions. Therefore, we do not present results using the overpass data sets and keep the number of different data sets and possible applied corrections to a surveyable level.

We denote the LER data set of TOMS flown on Nimbus 7 by "NIMBUS", and on Earth Probe as "EPTOMS". The term "OMILER" indicates the LER data set of OMI, and "OMIRCF" the radiative cloud fraction data set.

2.2 Ground-based UV irradiance

Daily sums of measured erythemally weighted UV irradiances were delivered by each site operator of eight low altitude UV radiation monitoring sites across Europe, see Fig. 1 and Table 2. The majority of these monitoring sites were selected in the SCOUT-O3 EC-project because of the availability of long-term quality controlled UV irradiance data. Data sets were re-evaluated in the context of the same project. Spectra are available at the European UV database, (http://uv.fmi.fi/uvdb) where, at submission, each spectrum undergoes an automatic quality flagging using the SHICrivm packages (Slaper et al., 1995) and the CheckUVspec package NILU, Norway (http://zardoz.nilu.no/~olaeng/CheckUVSpec/CheckUVSpec.html).

UV spectra are the basis of the produced daily sums for Bilthoven, Uccle, Jokioinen, Sodankylä, Potsdam and Lindenberg. For Thessaloniki, broadband data with a high temporal resolution (one measurement per minute) is used. The broadband data is calibrated against two collocated Brewer spectroradiometers. The Norrköping UV data set is fully broadband based; however, this data series was previously extensively re-evaluated, and relative spectral correction functions were applied. The main

AMTD
5, 61–96, 2012

characteristics of each monitoring site and references to operation protocols can be found in Den Outer et al. (2010). The measurement regime for all sites is from sunrise to sunset, with some variations in choice of tolerance.

The period prior to the onset of ground-based UV radiation monitoring is covered by modelled UV sums using ground-based measured data, with a minimum availability of measured total column ozone and GSI. This applies to the entire period covered by NIMBUS, for Thessaloniki until the 1980, Norrköping until 1984, and for Uccle until 2004. The modelled UV sums are taken from the so-called best estimate derived in Den Outer et al. (2010). In this paper, ground-based UV irradiance measurements and five different UV reconstruction models were inter-compared and a method was set up that delivered one best estimate of the historical ground level UV daily sums. The method takes into account the long-term stability and underlying agreement of the models, and the agreement with actual UV irradiance measurements. The models are thereby rescaled so that the calibration of the best estimate coincides with that of the measurements; the measurements are deemed to be the actual standard. Depending on the availability of model input data, the best estimates start well before the pre-satellite period for most sites, i.e. the mid sixties.

Data gaps occurring in the measured UV series after the onset of the UV radiation monitoring will not be supplemented with ground-based modelled data. Even so, data gaps in the best estimates (unavailable ozone or GSI data) will not be supplemented either. With respect to irradiance levels and distributions of daily UV sums, the residual differences between the best estimates and actual measurements are small, and much smaller than can be expected from a comparison of space-borne versus ground-based observations. Therefore, in the rest of the paper we will use "measured" to indicate both origins of the ground-based UV sums.

2.3 Ground-based global solar irradiance

The World Radiation Data Centre (WRDC) located in St. Petersburg, Russia, holds valuable data records of historical GSI-measurements (wavelength range

AMTD
5, 61–96, 2012

300–3000 nm) since the year 1964, when the data centre was founded. During a COST-726 action project (www.cost726.org), and in close collaboration with the WRDC staff, the daily sums of GSI for the European continent were extracted, quality checked and brought to the standard World Radiometric Reference scale if not already applied. The data set was made available within the community of the COST-project. We make use of this data set and have selected over 83 locations with sufficient data in the European continent. By "sufficient" we mean a data record covering more than three years, with over 50 % of the days per year available. Additional data for the period after 2004 and for a few African stations was extracted through direct access to the WRDC database. Only stations situated at altitudes below 750 m were chosen. The GSI data is transformed to cloud modification factors by applying the algorithm described in Den Outer et al. (2005), and indicated as F_{gb} in the rest of this paper. This algorithm is an empirically established relationship between measured and ground-based modelled daily UV sums. The relationship is dependent on classes of solar zenith angles and applied wavelength regimes.

Depending on the period considered, the total number and WRDC stations participating in this study may vary somewhat. We did not perform an additional quality control on top of what was already carried out at WRDC.

3 Optimal field of view

The agreement between any satellite-derived quantity and its ground-based measured counterpart will, among underlying intrinsic agreements, also be a function of the areas that are effectively intercompared. In our case, we expect an optimal agreement when the satellite pixels used for the CMF-calculation have a footprint or Field Of View (FOV) that is representative for the clouds drifting over the ground station during "mid day". The sky properties at mid day dominate because of the high solar elevation angle which delivers the largest portion of the total daily UV sum. An FOV that is too narrow will likely sample a non-representative fraction of the actual cloud layer. An FOV that is

AMTD
5, 61–96, 2012

too wide disregards the extremes due to the averaging in the first place and secondly, it incorporates clouds that in reality do not influence the UV irradiance at the particular ground station because of their location and wind direction/speed or may have dissolved at the time of arrival at the overhead location of the ground station. Similarly, the reverse applies for cloudless spots within the field of view.

The agreement of overpass data with a UV irradiance measurement at the time of overpass will not improve automatically when the FOV is narrowed. UV irradiance measurements have a large contribution of scattered radiation, even on cloudless days it is around 50 %, and a large area surrounding the site, 10–30 km, is of influence. The presence of clouds in the whole hemisphere is of importance and not only the clouds at zenith or in the direction of the sun. Decreasing the FOV would lead to assigning erroneously only the overhead clouds to be of influence.

We vary the number of satellite pixels included in the CMF calculations to investigate the existence of an optimal FOV for the application of LER data. The starting point is the LER value of the high resolution ($0.25^\circ \times 0.25^\circ$) OMI grid cell overhead the ground station. Next, we gradually increase the number of adjacent grid cells of which the LER values are averaged before entering the CMF calculation, and compare the accompanying UV sum with those measured at the ground stations. The result is shown in Fig. 2, as well as the result using the LER data on a $1.0^\circ \times 1.0^\circ$ grid. The number of grid cells in longitudinal direction is $1/\cos(\text{latitude})$ times the number of grid cells in latitudinal direction to perform the analysis on square areas. Therefore, the FOV is indicated by its size in degrees in the latitudinal direction. The ozone values are not varied and are taken from the ground-based observations. We have performed this analysis on the subset of concurrent days per site with respect to high and low resolution data sets.

An optimum occurs for an FOV of approximately 1.0–1.5°, where the averaged ratios of model to measured daily UV sums have minimum standard deviations. The increase of the standard deviations towards larger FOVs turns out to be independent of location of the ground-based stations. The Lindenberg data behaves a bit differently in this respect. The averaged level of the CMFs may vary with the considered field of view. Six

AMTD
5, 61–96, 2012

sites show an increase, while data of Lindenberg and Thessaloniki show a decrease with an increasing field of view. The averaged LER value for all WRDC-sites together turns out to be independent of the number of averaged adjacent grid cells. Hence, the above mentioned observation, which is also strongly influenced by the prevailing cloud regimes at each site, can be regarded as an artefact due to the subset of these eight sites.

An optimal FOV of 1.5° is quite a reasonable number because it corresponds to an area (170 x 170 km) that can be easily traversed by clouds during a few hours. We calculated the averaged wind speed of one year (2010) using the HIRLAM-6 meteorological fields at 1350 m a.s.l. (HIRLAM). The direction of the wind was disregarded in this calculation. Generally, the averaged speeds are higher above the sea west of Great Britain, i.e. 10–12 m s^{-1}, than above land, i.e. 6–10 m s^{-1}. For the eight locations of the UV radiation monitoring sites, the yearly averaged wind speeds range from 6.7 to 9.7 m s^{-1}; the smallest values were found in Finland and the highest in Bilthoven, Lindenberg and Potsdam. This means that clouds drift in about 5–7 h through the area set by the optimal field of view. Since the measurement of LER is close to local noon, it captures the clouds that contribute mostly to the reduction of the daily UV sum. The HIRLAM fields at 1350 m were chosen because 1350 m is right in the middle of the distribution of the cloud base height measured at Cabauw, a Meteorological site near Bilthoven. The distribution of the cloud base height is broad, almost flat up to 2 km (75 % is below 2000 m) and tails off to 10 000 m. We conclude that the current grid sizes of the LER data (1.0° × 1.0° and 1.0° × 1.5°) are a good, or even optimal, choice for calculating the cloud effect for daily UV sums.

AMTD
5, 61–96, 2012

4 Comparison

4.1 Spaceborne versus ground-based cloud modification factors

For all eighty WRDC stations, the corresponding spaceborne CMFs are calculated using the data sets NIMBUS, EPTOMS, OMILER and OMIRCF. We made plots of F_{gb} versus F_{sat} and show the results as density of data points in Fig. 3. In fact, we have plotted F_{gb} versus 1-LER (1-RCF for the lower right panel) thereby neglecting the enhancement of the irradiance due to ground reflections, which is at this point of minor importance. Since all CMFs apply to the UV wavelength range, we expect to observe linear relationships, i.e. the highest density along the line with slope 1 through the origin. The difference between the OMI instrument and the two TOMS instruments is striking. A linear relationship is indeed revealed in the EPTOMS and NIMBUS plots, while the plot of the OMILER based CMFs has a convex shape. The distributions of the LER values, shown in Fig. 4, also hint at a different behaviour of OMILER versus EPTOMS and NIMBUS. All LER distributions peak at a reflection of 0.08 and have an average value of 0.37 for the three instruments. However, the OMILER distribution has a yield of about 2.8 times higher than its yield at the average. The EPTOMS and NIMBUS distributions peak with a much lower maximum, only 1.6 times the level at the average. The grid size of OMILER, a little smaller than that of EPTOMS and NIMBUS, i.e. $1.0^{\circ} \times 1.0^{\circ}$ versus $1.0^{\circ} \times 1.5^{\circ}$, cannot explain this observation. Roughly the same distribution is found for OMILER when we apply a 4-point grid cell average (distant-weighted) prior to the calculation of the distribution.

The RCF data of OMI is, as expected, an entirely different quantity and contains a high percentage of clipped data: 18 % at RCF = 0 and 1.1 % at 1-RCF = 0. Still, it is obvious from the density plot of Fig. 3 that a useful relationship with F_{gb} can be derived.

The idea now is to determine the correlations, as they come forward in Fig. 3, and deduce empirical relationships that can be applied to improve the satellite derived CMFs. For computational reasons we must reduce the number of data points before we can enter any fitting procedure of an empirical relationship. The problem that emerges here

AMTD
5, 61–96, 2012

is that the skewed distributions of the CMFs do not allow a simple binning by averaging of CMF-intervals. Best results are eventually achieved by using the "mountain ridge" in the density plot to pin the correlation between spaceborne CMFs and ground-based CMFs. This procedure automatically disregards CMF pairs obtained on days with snow cover, i.e. high ground albedo, as these data points show up as outliers.

We first tested the existence of other hidden correlations by determining the ridges for different subsets of the data: i.e. grouping with respect to location, latitude, and SZA-intervals. SZA denotes the minimal solar zenith angle reached for the day and location of the considered data point. We made the density plots for latitude bands and for $10^\circ \times 10^\circ$ grid cells shown in Fig. 1. Only a dependency could be determined on the SZA for the shape of these density plots, i.e. the ridges. Thus for the European continent, it is sufficient to group data only with respect to the SZA. Trial and error lead to a most efficient set of SZA-intervals as given in Fig. 5. The first two SZA-intervals deliver the same ridge using NIMBUS and EPTOMS, and although the shape of the ridges is close to the ideal one-to-one relationship, there is room for small improvements. The shape of the ridges for the higher SZA boundaries deviates clearly from a straight line. Ridges produced using OMILER and OMIRCF are even more curved. Noticeable is the absence of an SZA-dependency of the RCF-curves.

We fitted 4th-order polynomials to the ridges and use these fit functions to correct LER and RCF values. In this way, we correct the satellite derived CMF such that it will yield, on average, the ground-based CMF constructed from GSI. Using 4th-order terms is rather over-dimensionalized but here we only want to establish a numerical expression for the found data ridges and do not develop a theory that would explain these correlations. Our ultimate goal is to improve on the spaceborne UV sums, and not understanding the optimal mathematical description of the correlations. For this reason, we do not list the determined eighty coefficients (4 instruments times 4 SZA intervals times 5 fit parameters), but they are available on request.

An additional correction was set up for OMIRCF to deal with the large subset of clipped data (18 %). The corresponding ground-based CMFs of this subset are plotted

AMTD
5, 61–96, 2012

as a function of the SZA in Fig. 6. A dependency on the SZA emerges, which is clearly visible for SZAs up to 55°; beyond 55° the scatter becomes too large. Data points causing the scatter were measured in winter and early spring. Therefore, it is most likely that these high reflections are attributed erroneously to snow cover, thereby resetting the cloud scattered fraction to zero while in reality the high reflection was caused by clouds, as follows from the low CMF delivered from the pyranometers readings.[1] Note that the error is usually made the other way around, i.e. high reflections due to snow are erroneously attributed to clouds leading to sever underestimations of the actual UV irradiances.

Triggered by previous results by Herman et al. (1999), Matthijsen et al. (2000), and Williams et al. (2004), which essentially state that the bare implementation of EPTOMS should lead to good results, we have setup an alternative correction scheme. Instead of correcting to the ideal one-to-one line, the EPTOMS-ridge obtained for the smallest SZA-interval is deemed the ideal curve describing the correlation between F_{gb} versus F_{sat}. Thus, we make all the other ridges EPTOMS-like. Correcting to the corresponding NIMBUS curve would have lead to the same results for that matter.

We test three ways of correcting the delivered LER (or RCF) values before these values enter the CMF-calculation:

1. uncorrected implementation
2. corrected to the one-to-one line
3. corrected to the curve found for the EPTOMS SZA1-interval

[1]RCF is a co-product of the effective cloud pressure and fraction using Raman Scattering (OMCLDRR), where also near real-time Ice and Snow Extent data, provided by the National Snow and Ice Data Center is included (http://acdb-ext.gsfc.nasa.gov/People/Joiner/OMCLDRR_README.htm). Data over snow/ice covered surfaces are flagged. Here it is mentioned that a value of "1" is then assigned to the RCF value instead of "0" as is the case in our retrieved data set.

AMTD
5, 61–96, 2012

The three implementations will be indicated by Uncor, Cor211 and Cor2A1 for the implementations 1, 2 and 3, respectively.

In Table 3, the result for the CMFs is summarized by the average of satellite versus ground-based derived CMFs. The average is calculated using the data from all WRDC ground stations. Obviously, the Cor211 leads to an average close to one, and the Cor2A1 leads to smaller values. The uncorrected OMILER produces a 9 % smaller value for the average F_{sat} compared to uncorrected NIMBUS and EPTOMS: 0.86, compared to 0.92 and 0.92, respectively.

4.2 Spaceborne versus ground-based UV sums

In Fig. 7, the effect in the UV wavelength range of the three implementations is shown by plotting the ratios of spaceborne to measured daily UV sums as a function of F_{gb}, the ideal algorithm should then be independent of this variable. A general algorithm to cope with high ground albedos is applied, using ancillary data on snow cover supplied by the site operators. A different SZA-interval is chosen in each panel for presentation reasons, where it should be mentioned that intervals for the smaller SZAs, if applicable, show better results, i.e. smaller scatter and closer to 1. The uncorrected implementation, shown in the insets of Fig. 7, leads generally to ratios smaller than 1 in all cases, as follows also from the shape and location of the ridges in Fig. 5. Implementation of Cor211 leads apparently to overestimation of the daily UV sums, especially at solid overcast. The best results were obtained with the Cor2A1-implementation, which was not anticipated. In Table 4, we list the averaged ratios of spaceborne to ground-based measured UV daily sums for the three implementations and all sites separately. Slightly improved overall results are indeed obtained for NIMBUS and EPTOMS, as shown by the "Cor2A1"-columns. The more Northern sites have benefited the most from the applied corrections. The results using OMILER and OMIRCF have undergone improvements of 10 %. The day-to-day variability, reflected in the listed standard deviations, improves only for OMIRCF: the other standard deviations are insensitive to the applied correction.

AMTD
5, 61–96, 2012

At this point we must note that the high resolution version of OMILER, used in Sect. 3, had been delivered using an earlier version of the LER algorithm, and as it turns out, can be used without corrections. Therefore, the results of Sect. 3, in particular Fig. 2, involve uncorrected high resolution LER data and corrected normal resolution LER data. Using the available high resolution version of OMIRCF instead of OMILER leads to a similar Fig. 2, however with a higher absolute level of the standard deviation. Of course, the correction for RCF data has to be applied to obtain this result.

Tables 5 and 6 list the averaged monthly and yearly sum ratios, respectively. Values using F_{gb} are given as well. Again, similar observations can be made for the performance of NIMBUS and EPTOMS on the one hand, and OMILER and OMIRCF on the other, where the latter have undergone a true improvement. Of course, for the winter half year NIMBUS and EPTOMS yield also too small monthly UV sums (October–February). This is the reflection of SZAs being large during winter and that only for large SZAs deviating correlations were found, cf. Figs. 3 and 5. Yearly sums – with relative small contribution of the winter half year – show only for OMILER and OMIRCF actual improvements of the averaged ratios. The standard deviations in the F_{sat} -derived monthly sums are larger than using F_{gb}, while for the yearly sums this again just holds for the OMILER and OMIRCF.

In Fig. 8, we illustrate the effect of the performed analysis on long-term time scales. The reductions of measured monthly UV sums have been calculated for all sites and are plotted simultaneously in this figure. The shown running means are based on averaging a number of reductions determined by the available monthly UV sums per year times the number of sites. Here the necessity to apply corrections is again brought to the fore. While the uncorrected LER-based F_{sat} do not follow the general trend inferred from the UV measurements, mainly due to OMILER, and would have indicated a downward trend, the corrected values follow the measured observation more closely and indicate an upward trend of the UV irradiance. The latter is in line with findings presented by Douglass et al. (2011).

AMTD
5, 61–96, 2012

5 Conclusions

We have analysed the performance of the Lambertian Equivalent Reflection of three consecutive spaceborne instruments when applied in algorithms to determine ground level ultraviolet irradiances. Also, the Radiative Cloud Fraction, a product of the Ozone Monitoring Instrument was considered. We made a comparison with CMFs derived from ground-based global solar radiation measurements from over eighty WRDC-stations and with UV irradiances measured at eight monitoring sites. Both comparisons lead to the observation that firstly, LER delivered by the TOMS instruments on Nimbus 7 and on Earth Probe require only small corrections and for large SZAs only, and secondly, that corrections are substantial for OMILER where a 10 % underestimation in the derived daily sums should be accounted for. The long-term analysis shows that uncorrected LER data could lead to a conclusion of a decrease of the UV irradiance in Europe, while the corrected version leads to the opposite. The latter is in line with findings based on pyranometer measurements and on UV irradiance measurements.

The overall best results were obtained unexpectedly with the correction that utilizes the initial correlation function between LER of the TOMS instrument of Earth Probe and ground-based cloud modification factors, i.e. the Cor2A1 implementation, and not the Cor211 implementation. This does not devaluate, however, the observation that the current calibration of the LER algorithm applied to OMI instrument produces deviating results compared to those produced by TOMS on Nimbus 7 and Earth Probe and the former LER calibration that has been used to produce the high resolution LER data set. The LER data sets of the TOMS instruments have quite a consistent performance with respect to the CMFs derived using the WRDC-dataset. This justifies the use of EPTOMS until the year 2002 for CMF-calculations and hence long-term trend analysis.

The radiative cloud fraction of OMI can be implemented to perform as a cloud effect proxy, although it is not intended as such. However, the drawback is that a substantial correction is needed and that quite a large percentage of clipped data exists in the

AMTD
5, 61–96, 2012

delivered data sets, although a found correlation with the SZA restores some of the actual variability in this subset.

The optimal field of view for daily UV sums calculations is 1–1.5° in latitudinal direction for the European continent; smaller or greater field of views lead to higher standard deviations in the comparison of satellite versus ground-based UV sums. This area is roughly comparable with the distance clouds traverse within 5–7 h over land.

Acknowledgements. Part of this work has been performed as part of the European Commission funded project SCOUT-O3 contract 505390-GOCE-CT-2004) and by the European Cooperation in Science and Technology (COST)-726. The work of A. V. Lindfors was funded by the Academy of Finland, decision 133259. We wish to acknowledge M. Brinkenberg from the Cabauw Experimental Site for Atmospheric Research, The Netherlands for the use of the cloud height measurements.

References

AURA Validation Centre: (former address http://avdc.gsfc.nasa.gov, last access: 1 July 2010), now the Space-Based Measurements of Ozone and Air Quality in the ultraviolet and visible, NASA Official, edited by: McPeters, R. D., http://ozoneaq.gsfc.nasa.gov/, last access: 9 December 2011.

Arola, A., Kazadzis, S., Lindfors, A., Krotkov, N., Kujanpää, J., Tamminen, J., Bais, A., di Sarra, A., Villaplana, J. M., Brogniez, C., Siani, A. M., Janouch, M., Weihs, P., Webb, A., Koskela, T., Kouremeti, N., Meloni, D., Buchard, V., Auriol, F., Ialongo, I., Staneck, M., Simic, S., Smedley, A., and Kinne, S.: A new approach to correct for absorbing aerosols in OMI UV, Geophys. Res. Lett., 36, L22805, doi:10.1029/2009GL041137, 2009.

Barnes, R. A., Eplee, R. E., Schmidt, G. M., Patt, F. S., and McClain, C. R.: Calibration of SeaWiFS, I. Direct techniques, Appl. Opt., 40, 6682–6700, 2001.

Bovensmann, H., Burrows, J. P., Buchwitz, M., Frerick, J., Noël, S., Rozanov, V. V., Chance, K. V., and Goede, A. P. H.: SCIAMACHY: mission objectives and measurement modes, J. Atmos. Sci., 56, 127–150, doi:10.1175/1520-0469(1999)056<0127:SMOAMM>2.0.CO;2, 1999.

AMTD
5, 61–96, 2012

Burrows, J. P., Weber, M., Buchwitz, M., Rozanov, V., Ladstätter-Weißenmayer, A., Richter, A., DeBeek, R., Hoogen, R., Bramstedt, K., Eichmann, K.-U., Eisinger, M., and Perner, D.: The Global Ozone Monitoring Experiment (GOME): mission concept and first scientific results, J. Atmos. Sci., 56, 151–175, doi:10.1175/1520-0469(1999)056<0151:TGOMEG>2.0.CO;2, 1999.

Calbó, J., Pagès, D., and González, J.-A.: Empirical studies of cloud effects on UV radiation: a review, Rev. Geophys., 43, RG2002, doi:10.1029/2004RG000155, 2005.

Den Outer, P. N., Slaper, H., and Tax, R. B.: UV radiation in the Netherlands: Assessing long-term variability and trends in relation to ozone and clouds, J. Geophys. Res., 110, D02203, doi:10.1029/2004JD004824, 2005.

Den Outer, P. N., Slaper, H., Kaurola, J., Lindfors, A., Kazantzidis, A., Bais, A. F., Feister, U., Junk, J., Janouch, M., and Josefsson W.: Reconstructing of erythemal ultraviolet radiation levels in Europe for the past 4 decades, J. Geophys. Res., 115, D10102, doi:10.1029/2009JD012827, 2010.

Douglass, A. and Fioletov, V.: Stratospheric ozone and surface ultraviolet radiation, in: Scientific Assessment of Ozone Depletion: 2010, Chapt. 2, Global Ozone Research and Monitoring Project-Report No. 52, World Meteorological Organization, Geneva, Swizerland, 516 pp., 2011.

Eck, T. F., Bhartia, P. K., and Kerr J. B.: Satellite estimation of spectral UVB irradiance using TOMS derived total ozone and UV reflectivity, Geophys. Res. Lett., 22, 611–614, doi:10.1029/95GL00111, 1995.

Eskes, H., van Velthoven, P., Valks, P., and Kelder, H.: Assimilation of GOME total ozone satellite observations in a three-dimensional tracer transport model, Q. J. Roy. Meteorol. Soc., 129, 1663–1681 doi:10.1256/qj.02.14, 2003.

Herman, J. R.: Global increase in UV irradiance during the past 30 years (1979–2008) estimated from satellite data, J. Geophys. Res., 115, D04203, doi:10.1029/2009JD012219, 2010.

Herman, J. R. and Celarier, E. A.: Earth surface reflectivity climatology at 340–380 nm from EP-TOMS data, J. Geophys. Res., 102, 28003–28011, 1997.

Herman, J. R., Krotkov, N., Celarier, E., Larko, D., and Labow, G.: Distribution of UV radiation at the Earth's surface from TOMS-measured UV-backscattered radiances, J. Geophys. Res., 104, 12059–12076, doi:10.1029/1999JD900062, 1999.

AMTD
5, 61–96, 2012

Herman, J. R., Labow, G., Hsu, N. C., and Larko, D.: Changes in cloud and aerosol cover (1980–2006) from reflectivity time series using SeaWiFS, N7-TOMS, EP-TOMS, SBUV-2, and OMI radiance data, J. Geophys. Res., 114, D01201, doi:10.1029/2007JD009508, 2009.

HIRLAM – HIgh Resolution Limited Area Model: Meteorological fields of http:/HIRLAM.org, last access: 9 December 2011, are parsed by the Royal Dutch Meteorological Institute (KNMI), to the National Institute for Public Health and the Environment, Bilthoven, The Netherlands, 2011.

ISCCP – The International Satellite Cloud Climatology Project: http://isccp.giss.nasa.gov/index.html, last access: 9 December 2011.

Kalliskota, S., Kaurola, J., Taalas, P., Herman, J., Celarier, E., and Krotkov, N. A.: Comparison of daily UV doses estimated from Nimbus-7/EPTOMS measurements and ground-based spectroradiometric data, J. Geophys. Res., 105, 5059–5062, 2000.

Kazadzis, S., Bais, A., Arola, A., Krotkov, N., Kouremeti, N., and Meleti, C.: Ozone Monitoring Instrument spectral UV irradiance products: comparison with ground based measurements at an urban environment, Atmos. Chem. Phys., 9, 585–594, doi:10.5194/acp-9-585-2009, 2009.

Kazantzidis, A., Bais, A. F., Gröbner, J., Herman, J. R., Kazadzis, S., Krotkov, N., Kyro, E., den Outer, P. N., Garane, K., Gorts, P., Lakkala, K., Meleti, C., Slaper, H., Tax, R. B., Turunen, T., and Zerefos, C. S.: Comparison of satellite-derived UV irradiances with ground-based measurements at four European stations, J. Geophys. Res., 111, D13207, doi:10.1029/2005JD006672, 2006.

Krotkov, N. A., Herman, J. R., Bhartia, P. K., Fioletov, V., and Ahmad, Z.: Satellite estimation of spectral surface UV irradiance 2. Effects of homogeneous clouds and snow, J. Geophys. Res., 106, 11743–11759, 2001.

Labow, G. J., Herman, J. R., Huang, L.-K., Lloyd, S. A., DeLand, M. T., Qin, W., Mao, J., and Larko, D. E.: Diurnal variation of 340 nm Lambertian equivalent reflectivity due to clouds and aerosols over land and oceans, J. Geophys. Res., 116, D11202, doi:10.1029/2010JD014980, 2011.

Levelt, P. F., Hilsenrath, E., Leppelmeier, G. W., van den Oord, G. H. J., Bhartia, P. K., Tamminen, J., de Haan, J. F., and Veefkind, J. P.: Science objectives of the ozone monitoring instrument, IEEE T. Geosci. Remote, 44, 1199–1208, doi:10.1109/TGRS.2006.872336, 2006.

Lindfors, A., Tanskanen, A., Arola, A., van der A, R., Bais, A. F., Feister, U., Janouch, M., Josefsson, W., Koskela, T., Lakkala, K., den Outer, P. N., Smedley, A. R. D., Slaper, H.,

AMTD
5, 61–96, 2012

and Webb, A. R.: The Promote UV Record: toward a global satellite-based climatology of ultraviolet irradiance, IEEE J. Sel. Top. Appl. Earth Obs. Remote Sens., 2, 207–212, doi:10.1109/JSTARS.2009.2030876, 2009.

Matthijsen, J., Slaper, H., Reinen, H. A. J. M., and Velders, G. J. M.: Reduction of solar UV by clouds: a comparison between satellite-derived cloud effects and ground-based radiation measurements, J. Geophys. Res., 105, 5069–5080, doi:10.1029/1999JD900937, 2000.

McKinley, A. and Diffey, B. L.: A reference action spectrum for ultra-violet induced erythema in human skin, in: Human Exposure to Ultraviolet Radiation: Risks and Regulations, Int. Congr. Ser., edited by: Passchier, W. F. and Bosnajakovich, B. F. M., Elsevier, New York, 83–87, 1987.

Slaper, H., Reinen, H. A. J. M., Blumthaler, M., Huber, M., and Kuik, F.: Comparing groundlevel spectrally resolved UV measurements from various instruments: a technique resolving effects of wavelenghtshifts and slitwidths, Geophys. Res. Lett., 22, 2721, 1995.

Tanskanen, A., Lindfors, A., Määttä, A., Krotkov, N., Herman J., Kaurola, J., Koskela, T., Lakkala, K., Fioletov, V., Bernhard, G., McKenzie, R., Kondo, Y., O'Neill, M., Slaper, H., den Outer, P., Bais, A. F., and Tamminen, J.: Validation of daily erythemal doses from ozone monitoring instrument with ground-based UV measurement data, J. Geophys. Res., 112, D24S44, doi:10.1029/2007JD008830, 2007.

UNEP: Environmental effects of ozone depletion and its interaction with climate change: 2010 assessment, United Nations Environmental Programme (UNEP), Nairobi, 278, 2010.

van der A, R. J., Allaart, M. A. F., and Eskes, H. J.: Multi sensor reanalysis of total ozone, Atmos. Chem. Phys., 10, 11277–11294, doi:10.5194/acp-10-11277-2010, 2010.

Van Dijk, A., den Outer, P. N., and Slaper, H.: Climate and ozone change effects on ultraviolet radiation and risks (COEUR). Using and validating earth observation, RIVM Report 610002001, available at: http://www.rivm.nl/bibliotheek/rapporten/610002002.pdf (last access: 9 December 2011), 2008.

Williams, J. E., den Outer, P. N., Slaper, H., Matthijsen, J., and Kelfkens, G.: Cloud induced reduction of solar UV-radiation: a comparison of ground-based and satellite based approaches, Geophys. Res. Lett., 31, L03104, doi:10.1029/2003GL018242, 2004.

WMO – World Meteorological Organization: Scientific Assessment of Ozone Depletion: 2010, World Meteorological Organisation, Geneva, Switzerland Global Ozone Research and Monitoring Project – Report No. 52, 438, 2011.

AMTD
5, 61–96, 2012

Table 1. Versions and retrieval date per satellite data, data was retrieved through ftp://toms.gsfc.nasa.gov.

Satellite	Version ID	Period	Retrieved or date created
NIMBUS*	L3, V8, NRT REFLECT GEN:04.119	1978–1993	2004-04-29
EPTOMS	L3, V8, NRT REFLECT GEN: 04.116	1996–2002	2004-04-26
OMILER	L3, JPM STD REFL340 GEN:06:089	2004–2008	2010-07-01
OMIRCF	L3, TO3 STD RCFGEN:09:154	2004–2008	2010-07-01
OMILER** (0.25° × 0.25°)	L3e, TO3 STD REFLECT, GEN:06:279	2004–2006	2009-04-12
OMIRCF (0.25° × 0.25°)	L3e, TO3 STD RCF GEN:09:155	2004–2008	2010-07-01

* The same version of the LER data set of NIMBUS and TOMS is now available at NASA http://ozoneaq.gsfc.nasa.gov/index.md, although it is now stored under "Radiative Cloud Fraction", LER data of OMI appears only accessible through ftp://toms.gsfc.nasa.gov.

** The high resolution version of LER was only available for a limited period of time and a limited measurement period (2004–2006); it was also generated with a different version of the retrieval algorithm.

AMTD
5, 61–96, 2012

Table 2. UV radiation monitoring sites.

Site ID, place, country	Lat., Lon., Height (Deg. dec.) (m)	Instruments	Used data
FIS, Sodankylä, Finland	67.36, 26.63, 179	Brewer MKII	04/1990–12/2006
FIJ, Jokioinen, Finland	60.81, 23.49, 107	Brewer MKIII	01/1996–12/2006
SEN, Norrköping, Sweden	58.58, 16.15, 43	RB SL501	03/1983–12/2008
DEP, Potsdam, Germany	52.36, 13.08, 107	Brewer MKII, MKIII	01/1995–04/2003
DEL, Lindenberg, Germany	52.21, 14.12, 127	Brewer MKIV,	01/1996–12/2004
		SPECTRO 320D	01/2005–12/2006
NLB, Bilthoven, The Netherlands	52.12, 5.19, 40	Broadband SL501	02/1994–12/1995
		Dilor 2XY.50	02/1996–12/2008
BEU, Uccle, Belgium	50.80, 4.357, 100	Brewer MKIII UV-Biometer 501	01/2004–12/2008
GRT, Thessaloniki, Greece	40.63, 22.95, 60	Broadband YES UVB-1 erythemal detector	08/1991–12/2006

AMTD
5, 61–96, 2012

Table 3. Averages of satellite-derived versus ground-based CMF for all WRDC ground stations.

Instrument	$\langle F_{sat}/F_{gb} \rangle$		
	Uncor	Cor211	Cor2A1
NIMBUS	0.92 ± 0.29	1.00 ± 0.32	0.94 ± 0.29
EPTOMS	0.92 ± 0.25	0.99 ± 0.28	0.94 ± 0.26
OMILER	0.86 ± 0.33	1.01 ± 0.38	0.96 ± 0.37
OMIRCF	0.82 ± 0.41	1.04 ± 0.39	0.98 ± 0.37

AMTD
5, 61–96, 2012

Table 4. Spaceborne versus ground-based measured daily UV sums, averaged ratios.

		NIMBUS			EPTOMS		
	Lat.	Uncor	Cor211	Cor2A1	Uncor	Cor211	Cor2A1
FIS	67.37	0.94 ± 0.22	1.04 ± 0.24	0.97 ± 0.23	0.95 ± 0.22	1.06 ± 0.23	0.98 ± 0.23
FIJ	60.82	0.96 ± 0.22	1.06 ± 0.25	1.00 ± 0.24	0.95 ± 0.26	1.03 ± 0.28	0.97 ± 0.27
SEN	58.58	1.06 ± 0.30	1.16 ± 0.35	1.09 ± 0.32	0.98 ± 0.25	1.07 ± 0.29	1.02 ± 0.27
DEP	52.36	0.95 ± 0.25	1.03 ± 0.28	0.97 ± 0.26	0.95 ± 0.27	1.04 ± 0.30	0.98 ± 0.28
DEL	52.21	0.93 ± 0.25	1.00 ± 0.27	0.95 ± 0.26	0.88 ± 0.23	0.96 ± 0.25	0.90 ± 0.24
NLB	52.12	1.00 ± 0.27	1.08 ± 0.29	1.02 ± 0.28	1.02 ± 0.33	1.11 ± 0.36	1.05 ± 0.34
BEU	50.80	0.99 ± 0.24	1.07 ± 0.26	1.01 ± 0.24	0.96 ± 0.25	1.05 ± 0.26	0.99 ± 0.25
GRT	40.63	0.97 ± 0.26	1.02 ± 0.27	0.98 ± 0.26	0.98 ± 0.22	1.03 ± 0.24	0.99 ± 0.22
ALL		0.97 ± 0.25	1.06 ± 0.28	1.00 ± 0.26	0.96 ± 0.25	1.04 ± 0.28	0.99 ± 0.26
		OMILER			OMIRCF		
	Lat.	Uncor	Cor211	Cor2A1	Uncor	Cor211	Cor2A1
FIS	67.37	0.86 ± 0.16	1.05 ± 0.18	0.99 ± 0.17	0.86 ± 0.41	1.05 ± 0.32	1.05 ± 0.27
FIJ	60.82	0.83 ± 0.24	1.01 ± 0.27	0.95 ± 0.26	0.86 ± 0.44	0.96 ± 0.41	1.06 ± 0.33
SEN	58.58	0.98 ± 0.27	1.18 ± 0.35	1.12 ± 0.32	0.89 ± 0.36	1.00 ± 0.32	1.12 ± 0.31
DEL	52.21	0.86 ± 0.24	1.02 ± 0.26	0.97 ± 0.26	0.77 ± 0.36	0.93 ± 0.30	0.97 ± 0.24
NLB	52.12	0.93 ± 0.23	1.10 ± 0.27	1.04 ± 0.26	0.81 ± 0.35	1.03 ± 0.33	1.05 ± 0.24
BEU	50.80	0.93 ± 0.26	1.11 ± 0.29	1.04 ± 0.28	0.77 ± 0.36	1.04 ± 0.35	1.04 ± 0.27
GRT	40.63	0.90 ± 0.22	1.01 ± 0.25	0.97 ± 0.24	0.85 ± 0.31	1.02 ± 0.27	0.97 ± 0.23
ALL		0.90 ± 0.23	1.07 ± 0.27	1.01 ± 0.26	0.83 ± 0.37	1.01 ± 0.33	1.05 ± 0.28

AMTD
5, 61–96, 2012

Table 5. Spaceborne versus ground-based measured monthly UV sums, averaged ratios for summer (April–September) and winter months (October–March).

F, Summer	NIMBUS	EPTOMS	OMILER	OMIRCF
GSI	1.02 ± 0.04	1.02 ± 0.05	1.04 ± 0.04	1.04 ± 0.04
Uncor	0.98 ± 0.06	0.98 ± 0.07	0.94 ± 0.05	0.91 ± 0.09
Cor211	1.03 ± 0.06	1.02 ± 0.07	1.04 ± 0.06	1.06 ± 0.06
Cor2A1	0.98 ± 0.06	0.98 ± 0.07	1.01 ± 0.05	1.01 ± 0.06
F, Winter				
GSI	1.01 ± 0.12	1.01 ± 0.08	1.06 ± 0.11	1.07 ± 0.11
Uncor	0.93 ± 0.12	0.89 ± 0.12	0.87 ± 0.16	0.87 ± 0.19
Cor211	1.03 ± 0.13	1.00 ± 0.12	1.05 ± 0.17	1.08 ± 0.16
Cor2A1	0.98 ± 0.13	0.95 ± 0.12	1.00 ± 0.17	1.03 ± 0.15

AMTD
5, 61–96, 2012

Table 6. Spaceborne versus ground-based measured yearly UV sums, averaged ratios.

F	NIMBUS	EPTOMS	OMILER	OMIRCF
GSI	1.01 ± 0.03	1.01 ± 0.03	1.04 ± 0.03	1.04 ± 0.03
Uncor	0.98 ± 0.03	0.97 ± 0.04	0.93 ± 0.04	0.89 ± 0.03
Cor211	1.03 ± 0.03	1.02 ± 0.04	1.04 ± 0.04	1.05 ± 0.04
Cor2A1	0.98 ± 0.03	0.98 ± 0.04	1.00 ± 0.04	1.00 ± 0.04

AMTD
5, 61–96, 2012

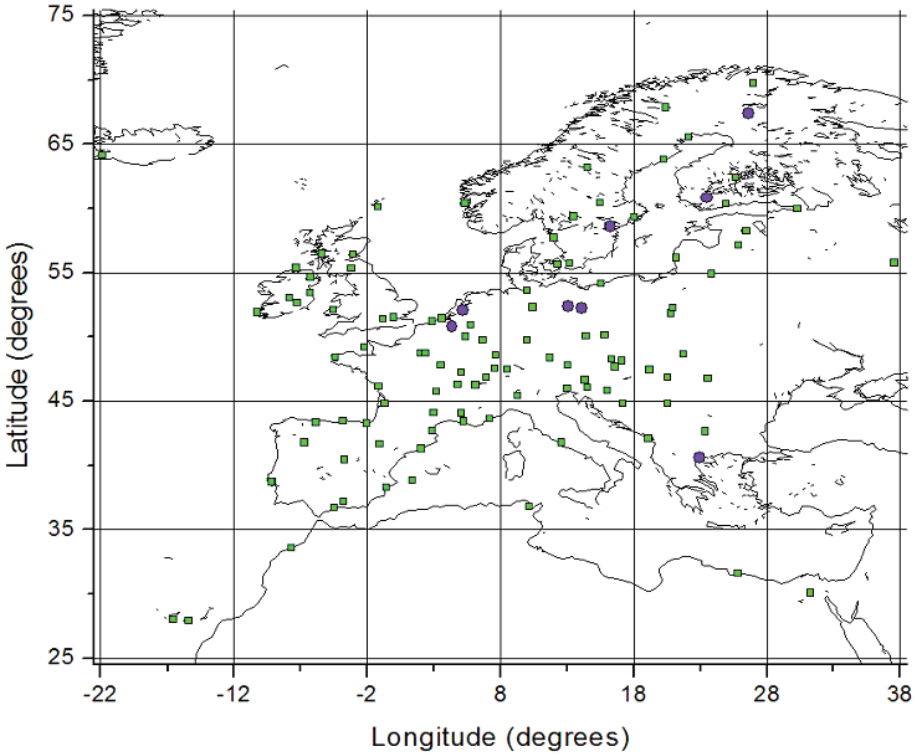

Fig. 1. Locations of WRDC stations (green squares) and UV monitoring stations (violet circles) in Europe, all UV monitoring stations are WRDC stations as well. Grid lines indicate the super grid cells used to determine underlying correlations.

AMTD
5, 61–96, 2012

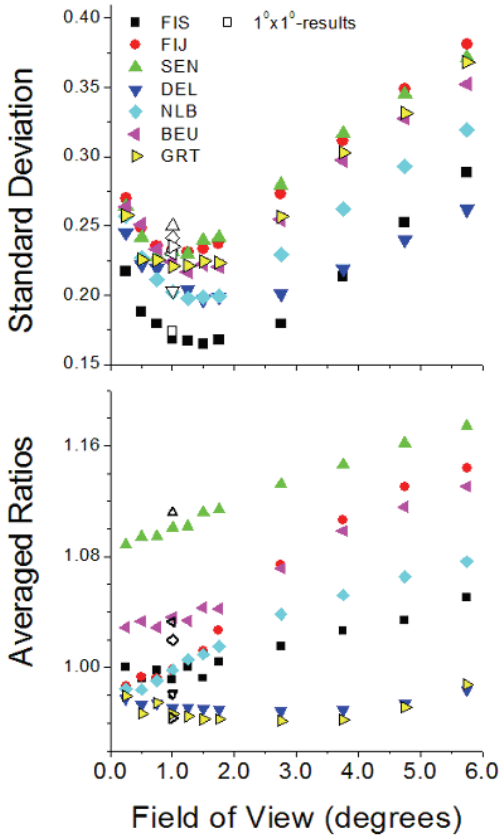

Fig. 2. Standard deviations (TOP) and averages (bottom) are plotted for ratios of spaceborne to measured daily UV sums for the OMI-period. Results are shown as a function of the field of view indicated by its size in the latitudinal direction. The FOV is square shaped. The results using the $1^{\circ} \times 1^{\circ}$-grid cells are shown as open symbols, key to monitoring sites is listed in Table 2.

AMTD
5, 61–96, 2012

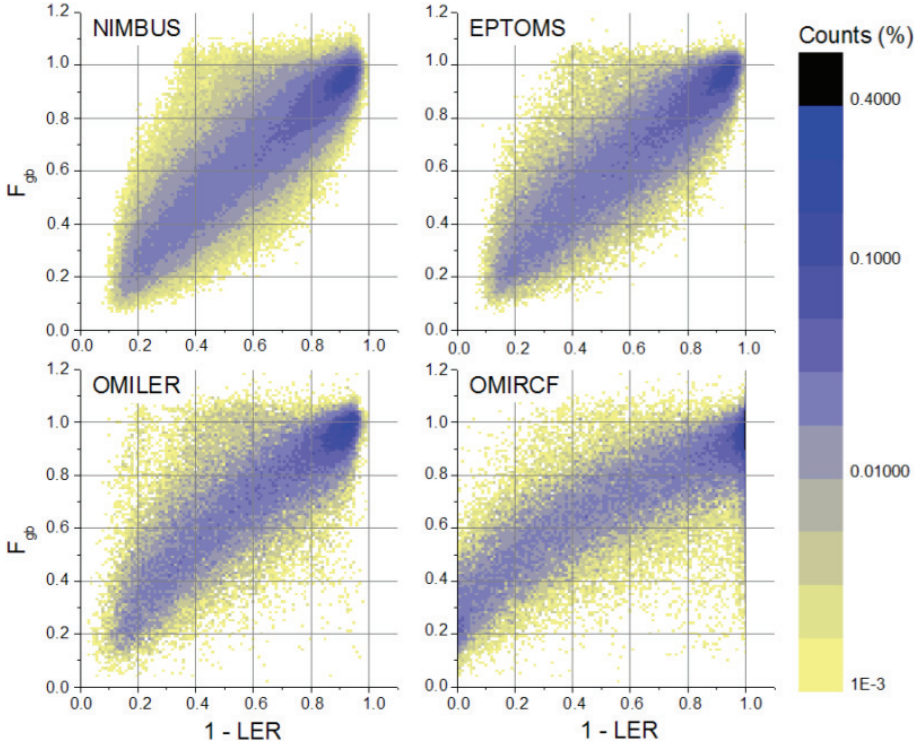

Fig. 3. Density plots of Cloud Modification Factors (CMF), F_{gb}, paired with co-located satellite-based Lambertian Equivalent Reflection (LER) measurements for the data sets indicated. Year-round data is shown; corrections for ground reflectivity (ground albedo) have not been applied.

AMTD
5, 61–96, 2012

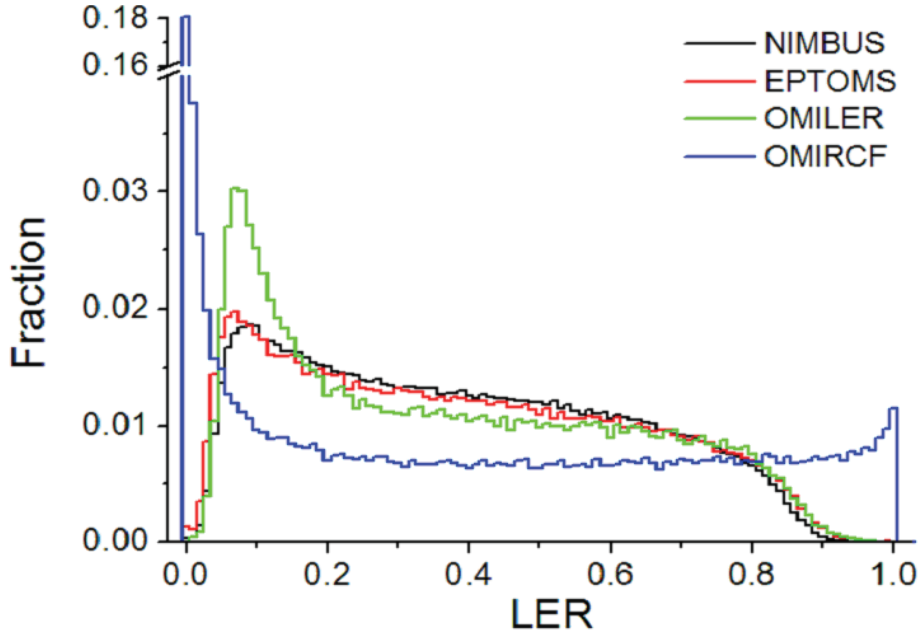

Fig. 4. The distributions of LER for satellites indicated are plotted. OMILER has a distribution that is more peaked, probably due to the initial 8 times better spatial resolution. The distribution of OMIRCF is shown also, this set has a high fraction of clipped data: 18 %.

AMTD
5, 61–96, 2012

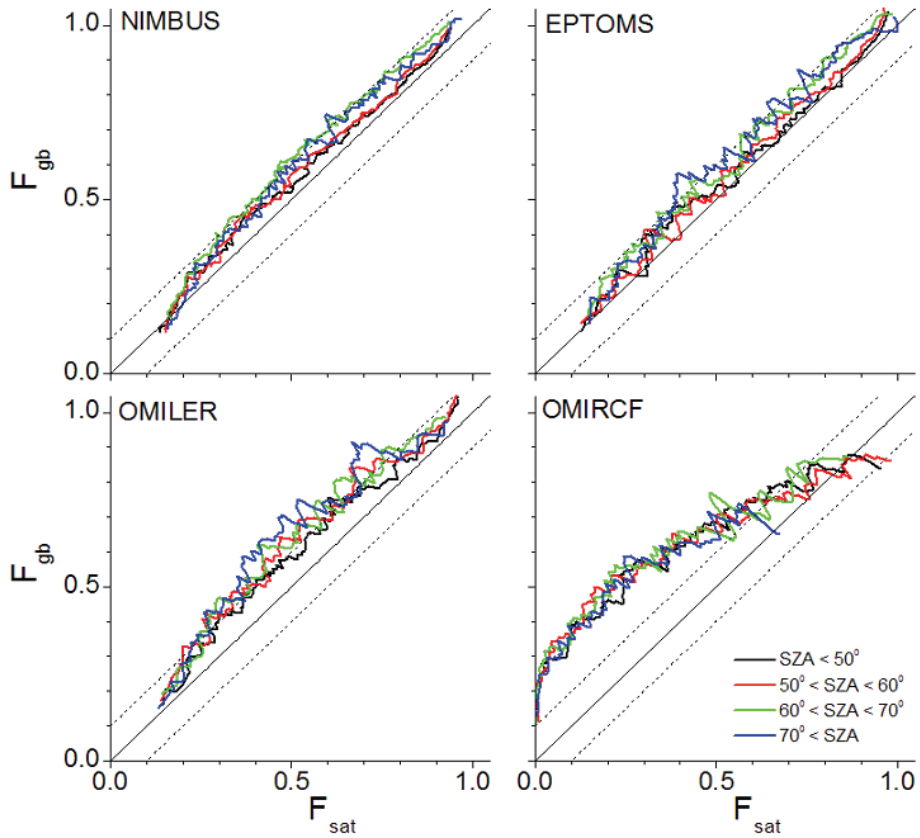

Fig. 5. The ridges of the density plots in Fig. 2 are shown. Data is grouped per SZA-interval, as indicated in the bottom right panel, and is the same for all 4 panels. The clipped data is omitted in the RCF-panel. Additional shifted $x = y$ grid lines are plotted to emphasize the observed differences between NIMBUS and TOMS on the one hand and OMILER and OMIRCF on the other.

AMTD
5, 61–96, 2012

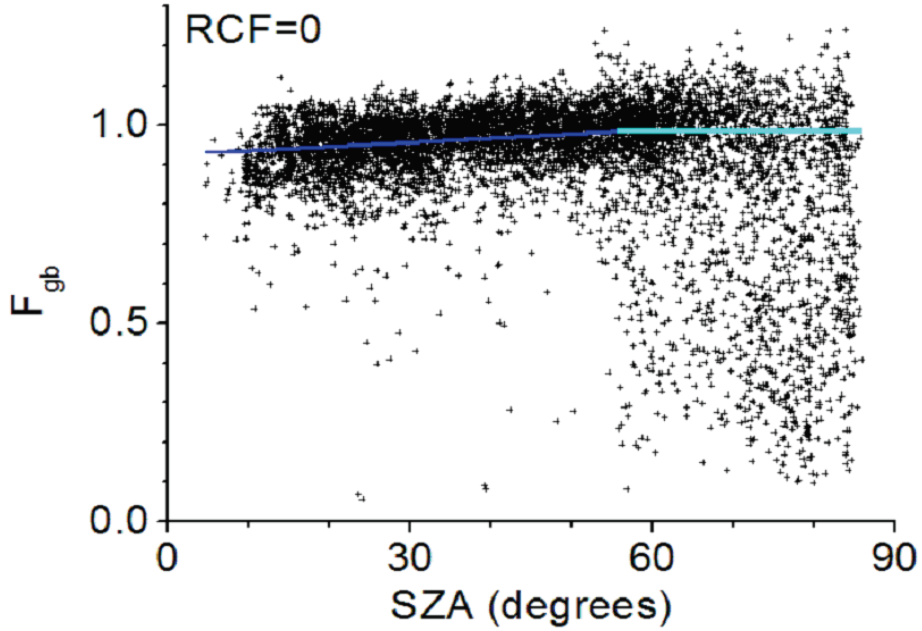

Fig. 6. The subset of ground-based CMFs for which RCF = 0 is plotted (black symbols) as a function of SZA. The implemented correction is shown as the blue line and applied for the SZA-interval 0–55°, for SZA greater than 55°, the level at 55° (0.984) is maintained (light blue). The scattered data points above 55°, were measured in the winter periods and are probable erroneously assigned snow covered ground-pixels instead of cloudy pixels.

AMTD
5, 61–96, 2012

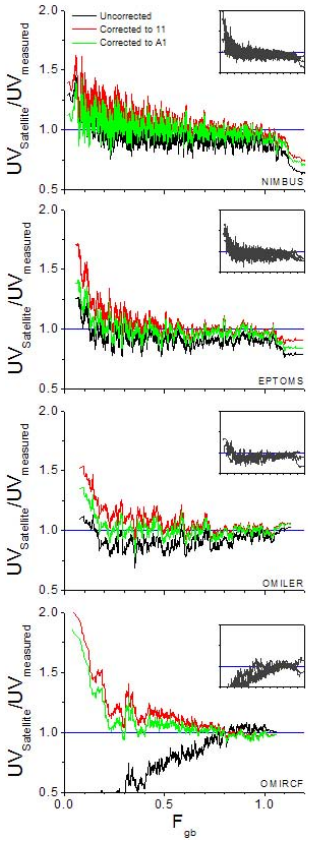

Fig. 7. Ratios of daily sums are plot as function of the ground-based CMF based on global solar radiation, 31-adjacent average are shown only. A different SZA-interval is chosen for presentation reasons in each panel. The SZA-interval are NIMBUS: 70° < SZA, EPTOMS: 60° < SZA < 70°, OMILER: 60° < SZA < 60°, OMIRCF: SZA < 50°. Insets show 31-adjacent uncorrected averages for all SZA-intervals.

AMTD
5, 61–96, 2012

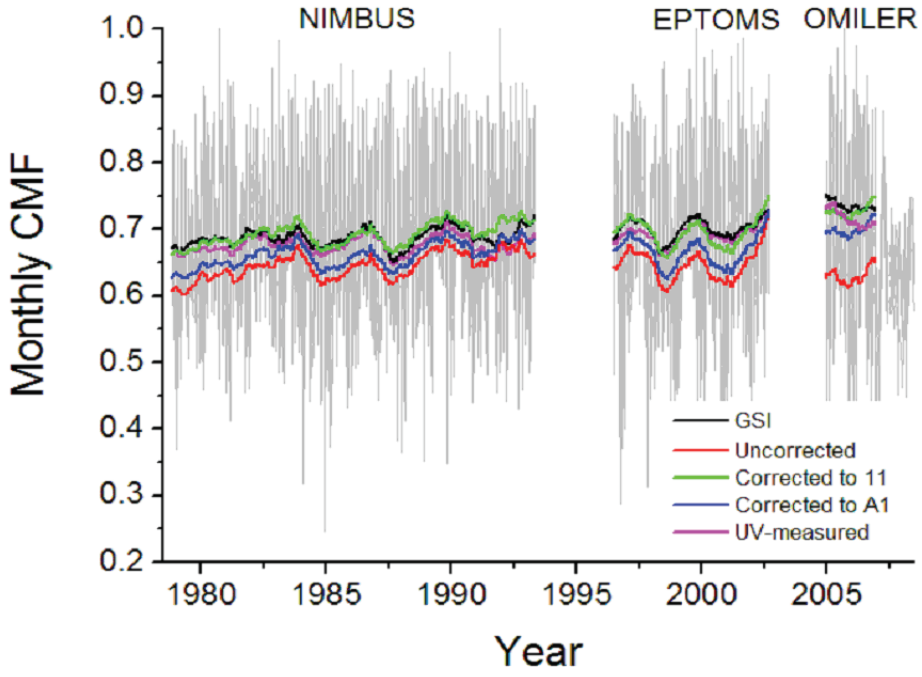

Fig. 8. Monthly average CMFs for all sites, grey. Running means are shown in colour as indicated by the legend. We calculated the running means until 2007, because afterwards, data is limited to 3 sites.

AMTD
5, 61–96, 2012